Preparation of inert polystyrene latex particles as microRNA delivery vectors by surfactant-free RAFT emulsion polymerisation

Cheuk Ka Poon[1], Owen Tang[2], Xin-Ming Chen[2], Binh T. T. Pham[1], Guillaume Gody,[3] Carol A. Pollock[2], Brian S. Hawkett*[1], Sébastien Perrier*[3,4]

[1] *Key Centre for Polymers & Colloids, School of Chemistry, Building F11, The University of Sydney, NSW 2006, Australia*

[2] *Kolling Institute of Medical Research, Royal North Shore Hospital and The University of Sydney, St Leonards, NSW 2065, Australia*

[3] *Department of Chemistry, The University of Warwick, Coventry, CV4 7AL, UK*

[4] *Faculty of Pharmacy and Pharmaceutical Sciences, Monash University, 381 Royal Parade, Parkville, VIC 3052, Australia*

Brian.hawkett@sydney.edu.au; s.perrier@warwick.ac.uk

Abstract

We present the preparation of 11 nm polyacrylamide-stabilised polystyrene latex particles for conjugation to a microRNA model by surfactant-free RAFT emulsion polymerisation. Our synthetic strategy involved the preparation of amphiphilic polyacrylamide-*block*-polystyrene copolymers, which were able to self-assemble into polymeric micelles and 'grow' into polystyrene latex particles. The surface of these sterically stabilised particles was post-modified with a disulfide-bearing linker for the attachment of the microRNA model, which can be released from the latex particles under reducing conditions. These nanoparticles offer the advantage of ease of preparation via a scaleable process, and the versatility of their synthesis makes them adaptable to a range of applications.

Introduction

Synthetic particles are a popular class of vectors for nucleic acid delivery. With the emergence of advanced synthetic techniques, these particles can be engineered to facilitate

non-viral nucleic acid delivery, targeting, cellular uptake and release.[1-3] Polymeric particles are attractive materials for such purposes. These structures can be built from the corresponding polymeric components in order to attain the desired properties and functionalities, such as particle size, charge, morphology and surface chemistry.[4-7]

Surfactant-free reversible addition-fragmentation chain transfer (RAFT) emulsion polymerisation technique is an advantageous method to synthesise latex particles for potential bioapplications,[8-10] since this approach does not required the use of particle-stabilising surfactants, which may desorb from particles overtime and hampered therapeutic applications.[11] To act as particle stabiliser in the preparation of latex particles by surfactant-free RAFT emulsion polymerisation, two strategies have already been employed: the use of surface-active amphiphilic RAFT-capped block copolymers,[12-16] or a one-pot polymerisation of a hydrophobic monomer from a low molar mass surface-active RAFT agent.[17] While the particles formation kinetics and their morphology control have been studied extensively, there are only a few scarce examples describing the use of this technique to engineer latex particles for the attachment of biomolecules or therapeutic agents. The most noteworthy examples to date are the work of Stenzel and co-workers, who prepared glucose-stabilised polystyrene latex particles as anti-infection agents,[18] and that of Wang and co-workers, who prepared poly(2-(dimethylamino)ethyl methacrylate)-stabilised redox-sensitive polystyrene latex particles as hydrophobic drug carrier.[19]

In this contribution, we demonstrate the synthesis of polystyrene (PS) latex particles as microRNA delivery vectors *via* surfactant-free RAFT emulsion polymerisation, using polyacrylamide (PAAm) as a particle steric stabiliser. On one hand, PS was chosen as the core-forming block for the particles since this inert material is suitable for a diverse range of biological applications.[20] For instance, PS nanoparticles have been used for modelling the

interactions of serum protein-nanoparticle complexes with cells.[21] Moreover, PS-based microspheres/microbeads have been employed for cell separation, immunoassays, drug delivery studies and biological imaging.[22] PAAm, on the other hand, is an attractive polymer because of its high solubility in aqueous media, its low susceptibility to hydrolysis at neutral pH and is non-toxicity.[23-25] It is also recognised as a potential material for therapeutic delivery and conjugation to genetic materials. For instance, Martínez-Ruvalcaba et al. prepared PAAm nanoparticle-based acrylic acid/chitosan hydrogel as a drug delivery model and studied its controlled release properties of ascorbic acid.[26] Maeda and co-workers demonstrated the successful conjugation of PAAm to single-stranded DNA for measuring the genetic variations between individuals of a species.[27] More recently, PAAm-stabilised iron oxide nanoparticles have been developed for the delivery of chemotherapy drugs into a solid tumour model.[28]

The synthesis of PAAm-stabilised PS latex particles has previously been reported by Xie and co-workers, who copolymerised styrene monomer droplets dispersed in aqueous phase with PAAm macro-RAFT agent to form 58 nm latex particles *in situ*.[29] Herein, we have designed a different surfactant-free RAFT emulsion polymerisation approach to prepare more uniform and smaller sized (11 nm) carboxyl-α-end HOOC-PAAm-stabilised PS latex particles, using pre-formed HOOC-polyacrylamide-*block*-polystyrene (HOOC-PAAm-*b*-PS) copolymer micelles as latex particle precursors. The use of an amphiphilic macro-RAFT agent permits to seed the particle formation and enables greater control over both the particle size, down to *ca* 10nm, and their size distribution, both of which are key to most bioapplications of nanoparticles as delivery vectors. We have used miR-200b duplex as model microRNA (miRNA) payload to illustrate the ability of the particle to carry and deliver an active agent. miR-200b has been shown to suppress epithelial-mesenchymal transition in human renal proximal tubular cells by decreasing the production of fibronectin-one of the major proteins involved in fibrosis when abundantly expressed.[30] The size of nanoparticles is particularly

relevant to the delivery of miR-200b, as it is targeted to human renal proximal tubular cells, a delivery process that is particularly known for requiring small delivery vectors. Indeed, delivery to human renal proximal tubular cells occurs through the glomerular filtration system, which is known to only allow through small particles, with a known cutoff of 14 nm, established by following protein pathways.[31] The conjugation of the miRNA duplex to the particles was achieved by first post-polymerisation functionalisation of the carboxyl-α-end functional particles with a bioreducible disulfide ligand 2-(2-pyridyldithio)ethylamine (PDE), followed by coupling to the thiol terminal group of the miRNA (Scheme 1).

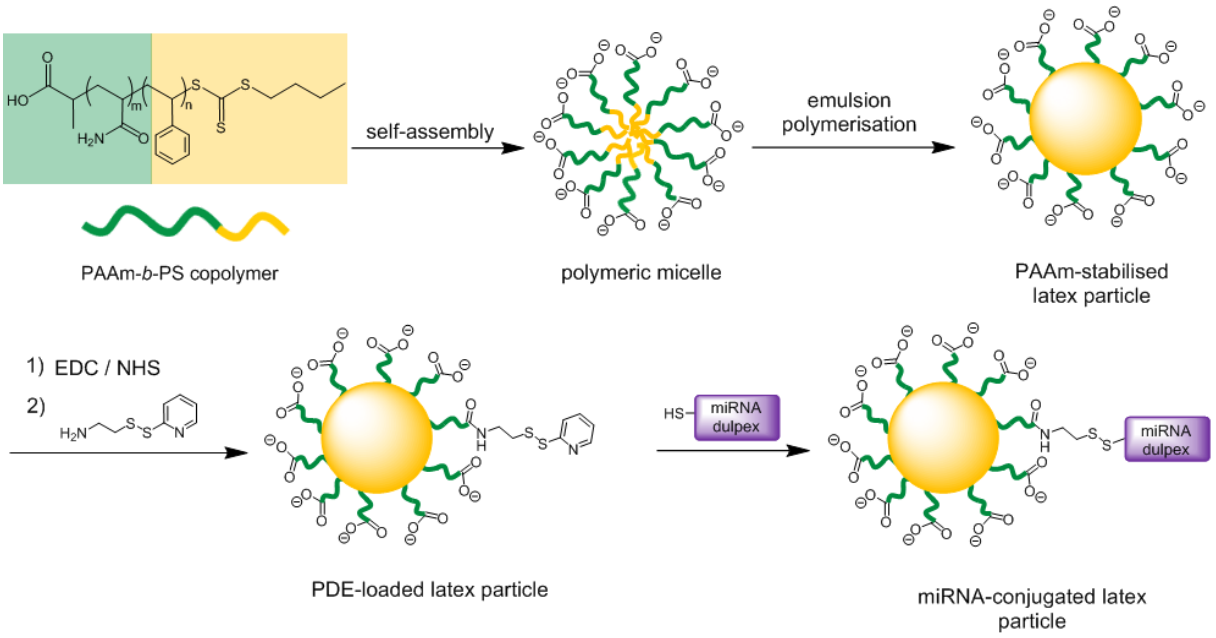

Scheme 1. Schematic summary of the particle engineering for miRNA conjugation: HOOC-PAAm-stabilised PS latex particle synthesis, post-polymerisation functionalisation with 2-(2-pyridyldithio)ethylamine linker and conjugation to miRNA.

Experimental

Materials. Chain-transfer agent (CTA) 2-(((butylthio)carbonothiolyl)thio)propanoic acid (called (propanoic acid)yl butyl trithiocarbonate (PABTC) in this paper) was provided by Dulux Group Australia. Acrylamide (AAm, 98+%, Sigma-Aldrich), 4,4'-azobis(4-

cyanovaleric acid) (V-501; Fluka), cysteamine hydrochloride (99+%, Sigma-Aldrich), Aldrithiol™-2 (98%, Sigma-Aldrich), *N*-(3-dimethylaminopropyl)-*N*′-ethylcarbodiimide hydrochloride (EDC, 98+%, purum, Sigma-Aldrich), *N*-hydroxysuccinimide (NHS, 99+%, Sigma-Aldrich), DL-dithiothreitol (DTT, 99+%, BioXtra, Sigma-Aldrich), tris(2-carboxyethyl)phosphine hydrochloride (TCEP·HCl, 98+%, Sigma-Aldrich), L-glutathione reduced (GSH, 98+%, Sigma-Aldrich), magnesium sulfate ($MgSO_4$, anhydrous, Merck), silica for column chromatography (40-63 μm; Grace Davison Discovery Sciences), sodium acetate buffer (NaOAc, 3M, pH 5.5, ultrapure, Affymetrix), UltraPure™ DNase/RNase-free distilled water (Thermo Fisher Scientific), sodium hydroxide (NaOH) pellets (Ajax Finechem), methanol for ESI-MS (MeOH, 99.80%, HPLC-grade, Merck), deuterium (D_2O, 99.90%, Cambridge Isotope Laboratories), deuterated chloroform ($CDCl_3$, 99+%) (Cambridge Isotope Laboratories) and deuterated dimethyl sulfoxide (DMSO-d_6, 99.5%, Cambridge Isotope Laboratories) were used as received. Styrene (99+%; Sigma-Aldrich) was purified by passing through a column of activated basic aluminium oxide (standard grade, 150 mesh, 58 Å; Sigma-Aldrich) to remove MEHQ inhibitor. 1,4-Dioxane (99+%; Merck) was purified by vacuum distillation. Water for reaction and particle dialysis was purified by Milli-Q® Integral Water Purification System (resistivity of water = 18.2 MΩ · cm at 25°C). 2-(*N*-Morpholino)ethanesulfonic acid (MES, 99+%, Sigma-Aldrich) buffer stock solution (100 mM, pH 5.65) was prepared with Milli-Q water and the pH was adjusted with aqueous NaOH (100 mM). Diethyl ether (Et_2O), ethyl acetate (EtOAc), MeOH and ethanol (EtOH, 70% and absolute) for reaction and purification were used as received. Disulfide-modified microRNA (miRNA)-200b duplex (sense: 5'-OH–$(CH_2)_6$–S–S–$(CH_2)_6$–UCAUCAUUACCAGGCAGUAUUUA[dT][dT]-3' and antisense: 5'-UAAUACUGCCUGGUAAUGAUGA-3', Sigma-Aldrich) was reduced by DTT to reveal the thiol group and purified according to the procedure described below.

Characterisation

Proton nuclear magnetic resonance (^{1}H-NMR) spectroscopy. NMR spectrometers (200 MHz and 300 MHz; Bruker Ultra Shield ™) were used for ^{1}H-NMR analysis. D_2O was used as the solvent for characterising HOOC-PAAm and PDE linker. DMSO-d_6 was used to analyse HOOC-PAAm-*b*-PS copolymer. $CDCl_3$ was used to characterise pyridinethione.

Electrospray ionisation mass spectrometry (ESI-MS). PAAm synthesised was characterized on Fourier transform ion cyclotron resonance (FTICR) mass spectrometer (Bruker Apex-Qe 7 Tesla) equipped with an Apollo II dual ESI/matrix-assisted laser desorption/ionization (MALDI) source, with the electrospray voltage set at 4.5 kV. Crude PAAm was dissolved in MeOH (HPLC grade)/H_2O (50:50, v/v) and run in negative ion mode *via* syringe pump. Mass spectra of PAAm were recorded in the range of 500-2000 m/z. PDE linker and pyridinethione synthesised were characterized on mass spectrometer detector (Finnigan™ LCQ™ Deca), using MeOH (HPLC grade) as the eluent at a flow rate of 0.2-0.4 mL / min and nitrogen as the sheath gas, with the electrospray voltage set at 4.5 kV and capillary temperature at 300 °C. Purified samples were dissolved in MeOH (HPLC-grade), making a final sample concentration of ~ 0.1 $mg \cdot mL^{-1}$. Samples were injected and run in positive ion mode.

Dynamic light scattering (DLS). Size distribution of micelles and PS latex particles was measured by dynamic light scattering (Malvern Zetasizer Nano). Particles were scatted by a helium-neon laser at 633 nm, 40mW and detected at an angle of 173 °. Samples were then filtered through 0.45 μm membranes, followed by equilibrating for 300 sec before measurement at 25 °C. Hydrodynamic diameter (d_H) and particle size distribution (PSD) of

micelles and latex particles were reported by intensity size distribution, which is obtained from correlation functions.

Hydrodynamic chromatography (HDC). Hydrodynamic volume (d_{vol}) of latex particles was determined by a Particle Size Distribution Analyser (PSDA; Polymer Laboratories). Dispersity of particles was accessed by the coefficient of variation (CV). Elution was performed on Type 2 cartridge, using PL-PSDA surfactant as the eluent (flow rate = 1.7 $mL \cdot min^{-1}$) and sodium 3-nitrobenzenesulfonate as the flow-rate marker. Samples were filtered through a 0.45 μm membrane before injection. The eluted samples were detected by a UV detector 254 nm. PS latexes standards (Duke Nanosphere™) were used for calibration.

Transmission electron microscopy (TEM). PS nanoparticles were observed using transmission electron microscope (Philips CM120 Biofilter, accelerating voltage 120 kV). Particle samples were diluted in water and the dispersion was drop-cast onto a 400 meshed-copper TEM grid. The grid has been coated with Formvar™, which was covered by a 10 nm carbon layer. Solvents from the sample on the TEM grid were evaporated before imaging under TEM.

Ultraviolet-visible (UV-Vis) spectroscopy. UV-Vis absorbance of PS latex particles, pyridinethione and microRNA in solution state were measured using UV-Vis-NIR spectrometer (Varian Cary 5000, Agilent) at room temperature. Samples were scanned in the range of 230-400 nm at 600 $nm \cdot min^{-1}$.

Preparation of UV-Vis calibration curve of pyridinethione. Pyridinethione was dissolved in water to various concentrations in the range of 4-170 μM. UV-Vis absorbance of the pyridinethione solutions at 342 nm was measured for constructing the standard curve, using water as the blank.

Procedures

Synthesis of macro-RAFT agent HOOC-PAAm. Macro-RAFT agent HOOC-PAAm was synthesised according to literature.[32] PABTC (0.81 g, 3.39 mmol), AAm (3.73 g, 52.4 mmol) and V-501 (0.10 g, 0.36 mmol) were dissolved in a mixture of 1,4-dioxane (6.62 g) and water (4.14 g). The reaction mixture was purged with nitrogen for 10 minutes, followed by stirring at 70 °C in an oil bath for 5 hours to give a clear, viscous and bright yellow liquid (AAm conversion = 93%, $M_{n,theo.} \approx 1300$ g·mol^{-1}, $M_{n,NMR} \approx 1400$ g·mol^{-1}, $DP_{NMR} \approx 14$). ^{1}H-NMR (200 MHz, D_2O, see Figure S1 for the protons attribution): δ (ppm) 0.95 (t, J = 9.2 Hz, 3H, RAFT 'Z' group CH_3), 1.20 (m, 3H, RAFT 'R' group CH_3), 1.37-1.98 (m, PAAm CH_2 backbone, RAFT 'Z' group CH_2, 2.07-2.67 (m, PAAm CH backbone, RAFT 'R' group CH), 3.44 (m, 2H, RAFT 'Z' group –CH_2–S–), 4.8 (bs, 1H, –CH–S–, under the HDO peak), 7.01 (bs, 2H, NH_2); ESI-MS characterisation confirmed the synthesis of well-defined HOOC-PAAm macro-RAFT agent (Figure S2).

Synthesis of HOOC-PAAm-*b*-PS diblock copolymer. HOOC-PAAm-*b*-PS diblock copolymer was prepared according to literature.[32] 1,4-Dioxane (10.86 g) and water (3.12 g) were added to the crude HOOC-PAAm macro-RAFT agent/dioxane/water solution (7.7 g of the solution above), followed by the addition of styrene (1.75 g, 16.8 mmol) and V-501 (0.18 g, 0.64 mmol). Note: the polymerisation mixture appeared to be slightly turbid during the degassing process (10 minutes degassing); this could possibly be due to the evaporation of dioxane, which caused the hydrophobic styrene monomer to phase-separate from the hydrophilic HOOC-PAAm/water layer. The polymerisation mixture became clear again when heated at 70 °C and remained clear throughout the reaction. The yellow solution was degassed under nitrogen for 10 minutes before stirring at 70 °C in an oil bath overnight, yielding a clear viscous and bright yellow liquid (styrene conversion = 90%, $M_{n,theo.}$ 2240 g·mol^{-1}, $M_{n,NMR}$ ≈ 2200 g·mol^{-1}, $DP_{Sty,NMR}$ ≈ 8). ^{1}H-NMR (200 MHz, DMSO-d_6, see Figure S4 for the protons attribution): δ (ppm) 0.84 (m, 3H, RAFT 'Z' group CH_3), 1.04 (m, 3H, RAFT 'R' group CH_3), 1.18-2.42 (m, PS and PAAm CH and CH_2 backbone, RAFT 'Z' group CH and CH_2, RAFT 'R' group CH), 3.20 (m, 2H, RAFT 'Z' group –CH_2–S–), 6.29-7.38 (m, aromatic ring of PS). Styrene conversion and molecular weight distribution of diblock copolymer are summarised in **Error! Reference source not found.**.

Synthesis of PS latex particles. The crude HOOC-$PAAm_{14}$-*b*-PS_8 diblock copolymer dioxane/water solution above (1.00 g) was charged into a round-bottom flask and stirred continuously. Aqueous NaOH (0.3% w/w, 1.94 g, 0.15 mmol) was added to the stirring diblock copolymer solution, followed by dropwise addition of water (22.10 mL at 0.02 mL·min^{-1}) to give a clear yellow micelle solution. After the addition of styrene monomer

(0.06 g, 0.60 mmol), the solution was stirred vigorously for 30 minutes at room temperature.V-501 (0.030 g, 0.11 mmol) and NaOH (3% w/w, 1.08 g, 0.81 mmol) were added to the solution, followed by stirring for a further 2 hours. The solution was then degassed under nitrogen for 15 minutes and heated in an oil bath at 70 °C for an hour. Conversion of styrene was determined by gravimetric analysis to be 99%. The particles were purified by dialysis against Milli-Q water (MW cut-off = 2000 $g \cdot mol^{-1}$). Solids content of particles after dialysis was established to be 0.37%. Size and dispersity of PS latex particles were obtained from DLS and HDC. The latex particles were also studied by TEM.

PS latex particle stability in freeze-thaw cycles. PS latex particles were frozen by dry ice for an hour, followed by thawing at room temperature. The freeze-thaw procedure was repeated 10 times and the PSD of latex was monitored by DLS at the end of each thawing.

Synthesis of 2-(2-pyridyldithio)ethylamine (PDE) linker. 2-(2-Pyridyldithio)ethylamine (PDE) linker was synthesised according to literature.[33] Briefly, cysteamine · HCl (0.1315 g, 1.16 mmol) was dissolved in a solution of Aldrithiol™ -2 (0.694 g, 3.14 mmol) in MeOH (2.57 mL). The clear yellow solution was stirred at room temperature for 20 hours under nitrogen. The product was purified by precipitation in Et_2O. Precipitates were collected by vacuum filtration and washed by Et_2O until the filtrate became colourless. The white solid obtained was dried under reduced pressure at 40 °C overnight to yield 0.202 g (78%). The Et_2O layers were reserved for the synthesis of pyridinethione. ^{1}H-NMR (200 MHz, D_2O, see Figure S5 for the protons attribution): δ (ppm) 3.06-3.12 (t, J = 6.0 Hz, 2H, –C<u>H</u>$_2$–NH_2), 3.30-3.36 (t, J = 6.0 Hz, 2H, –S–CH_2–), 7.29-7.35 (t, J = 6.0 Hz, 1H, pyridyl ring CH at 5-position), 7.72-7.86 (m, 2H, pyridyl ring CH at 3- and 4-position), 8.43-8.46 (d, J = 6.0 Hz, 1H, pyridyl ring CH at 6-position). ESI-MS (m/z) for $[C_7H_{10}N_2S_2+H]^+$ = 187, theoretical m/z = 186.0285.

Synthesis of pyridinethione standard. Pyridinethione standard was prepared according to the reported protocol.[33] Et_2O layers (containing unreacted Aldrithiol™ -2 and pyridinethione) obtained from the purification procedure of PDE linker described above were combined and concentrated under vacuum. The residue was dissolved in MeOH (20 mL) and mixed with cysteamine · HCl (0.3540 g, 3.12 mmol) to form a cloudy orange yellow solution. The turbid solution was stirred at room temperature for 20 hours under nitrogen. EtOAc (20 mL) was then added to the turbid solution, followed by washing with Milli-Q water (2 × 20 mL). The extracted EtOAc layer was dried by $MgSO_4$ and filtered. The filtrate was concentrated and the residue was purified by silica column chromatography (Purified pyridinethione R_f (EtOAc) = 0.45-0.5). The purified product was dried under reduced pressure at 40 °C overnight to yield a dark orange solid. ^{1}H-NMR (300 MHz, $CDCl_3$, see Figure S6 for the protons attribution):): δ (ppm) 6.78-6.82 (t, *J* = 6.0 Hz, 1H), 7.39-7.45 (m, 1H), 7.58-7.63 (m, 2H). ESI-MS (m/z) for $[C_5H_5NS+H]^+$ = 112, theoretical m/z = 111.0143.

Synthesis of PDE-conjugated PS latex particles. PS latex (solids content = 0.37%, 2 mL) was dispersed in MES buffer (100 mM, pH 5.65, 1.7 mL), followed by mixing with EDC (0.015 g, 0.080 mmol), NHS (0.0184 g, 0.160 mmol) and aqueous PDE linker solution (4.72 mM, 0.3 mL, 1.42 μmol) at room temperature overnight. The latex particles were then purified by dialysis against Milli-Q water (MW cut-off = 2000 $g \cdot mol^{-1}$). The solids content of the modified particles after dialysis was established to be 0.30%. Size and dispersity of the PDE-conjugated particles was checked by DLS and HDC.

Quantification of PDE loading on PS latex particles. Purified PDE-loaded PS latex particles (0.5 mL) was first diluted with Milli-Q water (0.5 mL) and mixed with aqueous TCEP solution (70 mM, 5 μL). The release of pyridinethione upon disulfide reduction by

TCEP was monitored *in situ* by the increase in absorbance at 342 nm until constant absorbance was reached. Water was used as the blank for absorbance measurement.

Conjugation of microRNA to PDE-loaded PS latex particles. miR-200b duplex was dissolved in DNase/RNase-free distilled water (0.133 mM, 30 μL, 4 nmol) and incubated with aqueous DTT solution (100 mM, 32 μL) at room temperature for 2 hours. The miRNA was extracted by mixing the solution with NaOAc (3 M, pH 5.5, 8 μL), followed by the addition of EtOH (absolute, 205 μL). The solution was incubated at -80 °C for 1 hour before centrifugation at 16,000 g for 30 minutes at 4 °C. The miRNA pellet was resuspended in EtOH (70%, 205 μL) and centrifuged at 16,000 g for 10 minutes at 4 °C. The purified thiol-capped miRNA pellet was dried under reduced pressure and mixed with purified PDE-loaded PS latex (solids content = 0.30%, 100 μL) at room temperature. The reaction was monitored *in situ* by the increase in absorbance at 342 nm until a constant absorbance was reached. The miRNA-conjugated PS latex particles were purified by ultrafiltration (MW cut-off = 30,000 $g \cdot mol^{-1}$) for at least 5 times. The presence of unreacted miRNA and pyridinethione being washed out was monitored by measuring the absorbance of the filtrates at 260 nm and 342 nm respectively. The attachment of miRNA onto PS latex particles was confirmed by the absorbance of the purified retentate at 260 nm and 310 nm. Water was used as the blank for all UV-Vis absorbance measurements.

Release of conjugated miRNA from PS latex particles. Purified miR-200b-PS latex particle conjugates (solids content = 0.30%, 50 μL) dispersed in DNase/RNase-free distilled water (160 μL) was incubated with aqueous GSH solution (33 mM, 90 μL, final concentration for incubation = 10 mM) at room temperature. At 30 min and 60 min incubation, the PS latex was washed by ultrafiltration (MW cut-off = 30,000 $g \cdot mol^{-1}$). The release of miRNA was

confirmed by the increase in absorbance of the filtrates and the decrease in absorbance of the retentates at 260 nm. Water was used as the blank for all UV-Vis absorbance measurements.

Results and discussion

HOOC-PAAm-*b*-PS diblock copolymer preparation. The carboxyl-α-end HOOC-PAAm-*b*-PS diblock copolymer was prepared *via* a two-step RAFT polymerisation process. This was achieved by first polymerising AAm to generate a HOOC-PAAm macro-RAFT agent, followed by block extension with styrene monomer. The HOOC-PAAm macro-RAFT agent was prepared by polymerisation of AAm mediated by the chain transfer agent (CTA) PABTC in a mixture dioxane/water (60:40 v:v). Despite water being an excellent solvent for AAm monomer and PAAm,[23,34] a number of side reactions have been reported in the homopolymerisation of AAm in pure water or buffer, especially when mediated by dithioester CTAs. These side reactions include hydrolysis of the monomer to form ammonia, which causes unwanted aminolysis of the CTAs, slow polymerisation rate and poor monomer conversion (< 28%).[35-37] Aiming to minimise such side reactions, we opted for a trithiocarbonate CTA, PABTC, to mediate the polymerization, as it has better hydrolytic stability even at temperatures as high as 70 °C,[24] and the polymerisations were undertaken in 40% in volume dioxane, in order to limit AAm hydrolysis. Furthermore, dioxane also facilitates the solubilisation of both PABTC and styrene monomer at the chain extension step.[38, 39] Polymerisation of AAm was carried out for 5 hours. The polymerisation solution remained clear and bright yellow in colour throughout the reaction, suggesting that the PAAm remained well-dissolved in the co-solvent mixture and that the degradation of the trithiocarbonate end group remains negligible. Monomer conversion and DP_{AAm} were determined from ^{1}H-NMR *in situ* by comparing the integration of the PAAm backbone (from 1.37 to 2.67 ppm) with the terminal methyl group of the RAFT agent Z group (0.95 ppm) used as internal reference (Figure S1 in ESI). The polymerisation proceeded to > 95% conversion, to yield a macro-RAFT agents of 14 AAm units. Retention of both the COOH and the trithiocarbonate groups were verified by ESI-MS analysis (Figure S2 in ESI), which

revealed two populations, corresponding to single- and double-charged species. The single-charged population corresponds to HOOC-PAAm with the trithiocarbonate end group, of DP ranging from 5 to 21 units and a central peak at m/z = 1231.5, corresponding to HOOC-$PAAm_{14}$, which is in good agreement with the DP obtained from ^{1}H-NMR analysis.

The block extension with styrene was performed in batch by adding styrene monomer, dioxane and initiator to the AAm polymerisation solution. The co-solvent ratio of dioxane/water had to be tuned (i.e. from 60:40 to 70:30 v:v) to solubilize both styrene and HOOC-PAAm macro-RAFT agent and obtain a homogeneous and clear reaction solution. Conversion and DP of styrene were determined from ^{1}H-NMR *in situ* (Figure S4). Comparing the integration of the aromatic protons of PS backbone with the vinyl peaks of the styrene monomer at 5.81 ppm gave 88% monomer conversion, equivalent to a styrene DP around 8. Unfortunately, the diblock copolymer HOOC-$PAAm_{14}$-*b*-PS_8 could not be analysed by size exclusion chromatography and ESI-MS due to its poor solubility.

Preparation of PS latex particles stabilised by PAAm. PS latex particles stabilised by PAAm were prepared *via* surfactant-free RAFT emulsion polymerisation. This involved the self-assembly of HOOC-$PAAm_{14}$-*b*-PS_8 diblock copolymer into polymeric micelles, followed by chain-extending the hydrophobic block within the micelle cores with additional styrene monomer. Dioxane was added to the solution as a co-solvent for the self-assembly of PAAm-*b*-PS, as it enables better mobility of the glassy PS block.[39] Micellization was performed by first adding the crude HOOC-$PAAm_{14}$-*b*-PS_8 diblock mixture to an aqueous NaOH solution, followed by slow addition of water with constant stirring. NaOH deprotonates the carboxylic acid group at the chain end of the macroRAFT surfactant, thus promoting ionisation between PAAm chains for micelization. It is noteworthy that attempts to form micelle in absence of NaOH were unsuccessful. Upon addition of water to the copolymer solution, the hydrophobic

styrene block aggregated into micelle cores along with the butyl trithiocarbonate end group; the hydrophilic PAAm block and the carboxylic acid moiety became the coronas of the micelles and extended in the aqueous environment. The micelle solution was observed to be clear throughout the addition of water, indicating the micelles were well dispersed in the water phase. The size distribution of the micelles was confirmed by DLS. Figure 1 shows the micelles having an average size of 9.3 nm in diameter, with a particle size distribution (PSD) of 0.216. It is noteworthy that the approximate micelle radius (4.7 nm) was comparable to the theoretical length of a single fully-stretched $PAAm_{14}$-*b*-PS_8 copolymer chain (22 monomer units × 0.25 nm = 5.5 nm).

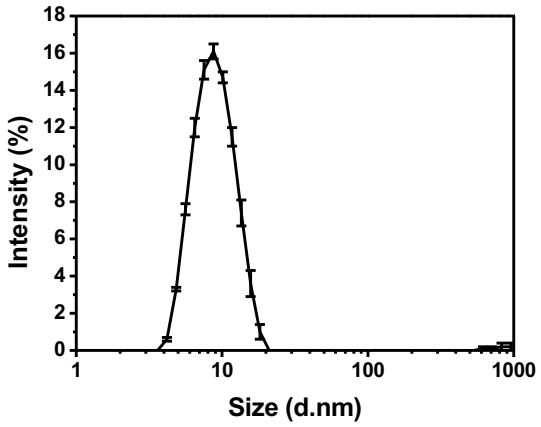

Figure 1. Size distribution of micelles from the self-assembly of ^{-}OOC-$PAAm_{14}$-*b*-PS_8 obtained by dynamic light scattering.

RAFT emulsion polymerisation was carried out with the addition of styrene monomer to the micelle solution. The solution became a homogeneous turbid dispersion after vigorous stirring, suggesting that the styrene monomer was well-dispersed in the aqueous phase, while some of the monomer might have penetrated into the polymeric micelle cores. Addition of V-501 initiator was accompanied by aqueous NaOH to deprotonate the carboxylic acid groups to insure a complete dissolution in the aqueous phase. The reaction fed with styrene monomer appeared to be less turbid and eventually became clear yellow as polymerisation proceeded.

This indicates both the depletion of styrene monomer in the aqueous phase and that particle formation was taking place. At the end of the reaction, particles were dialysed against Milli-Q® water to remove unreacted styrene monomer (less than 1% remaining after polymerisation), initiator and dioxane. The removal of dioxane was essential to prevent any free exchange of the chain-extended diblock copolymer chains between the final latex particles. The size distribution of the purified PS latex particles was analysed by hydrodynamic chromatography (HDC) and confirmed by DLS (Figure 2). HDC is an excellent technique to obtain accurate information on the size of the particles, and the monomodal distributions observed indicate the particles were uniform in size in general without the presence of large aggregates, as confirmed by their relatively low coefficient of variation (CV) values (Table 1). DLS confirmed these observations, and TEM images (Figure 3) reveal the particles are spherical in shape and also confirmed a fairly uniform size. The observed particle morphology correlated with the structure of their precursor micelles formed by $PAAm_{14}$-*b*-PS_8 copolymers was suggested to be spherical from DLS (Figure 1) as discussed above. TEM results also supported that chain-extension of the diblock macro-RAFT agents with styrene was carried out within the loci of spherical micelles, which have been evolved into spherical particles. Table 1 summarises the sizes of particles obtained from different techniques. Diameters of the particles measured from DLS were in good agreement with the results obtained from HDC. The overall particle diameters estimated from TEM appeared to be smaller compared to DLS and HDC measurements as anticipated, since TEM only images the electron-rich PS core of the particles. The PAAm chains at the particle corona, on the other hand, were not electron-dense enough to be observed under the electron microscope without staining. Furthermore, the PS chains at the particle cores were expected to collapse when the latex particles were dehydrated during TEM sample preparation. In

addition to the water evaporation process, electron bean irradiation during TEM imaging could also cause the particles to shrink from their original dimensions.[40-42]

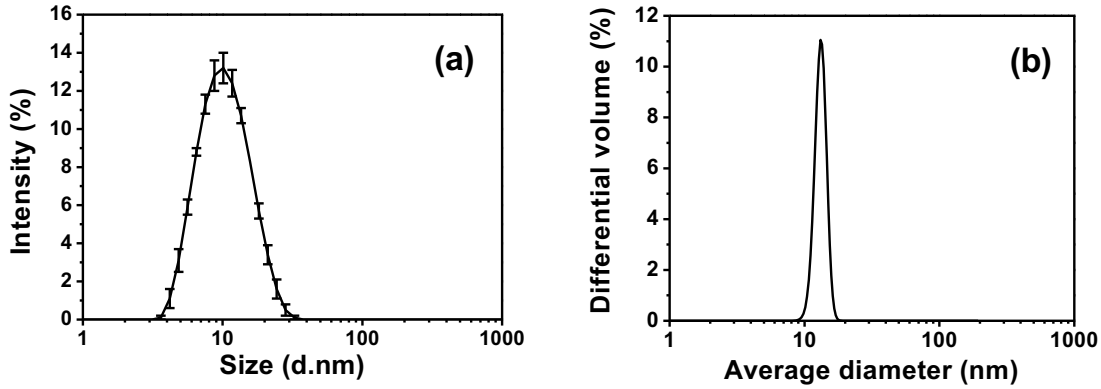

Figure 2. Size distributions of PAAm-stabilised PS latex particles measured by (a) DLS and (b) HDC.

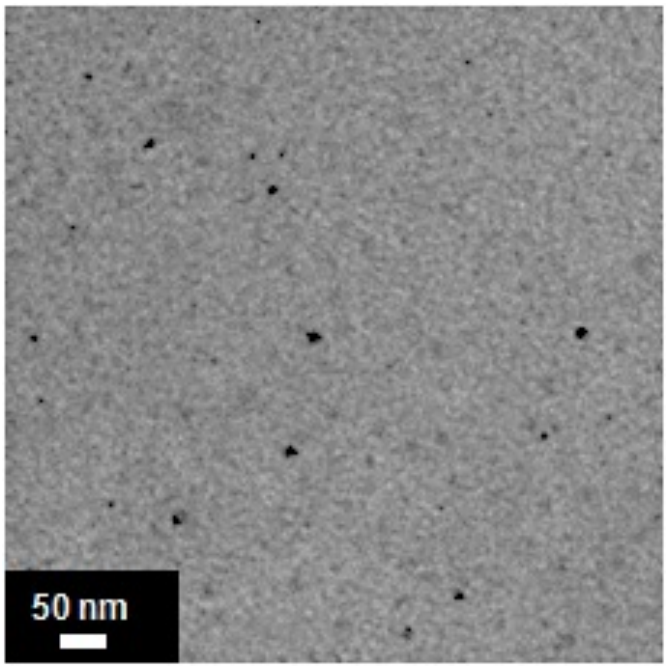

Figure 3. TEM image of PS latex particles stabilised by PAAm.

Table 1. Size and dispersity of PS latex particles obtained from different techniques

PS latex particle diameter (nm)			Particle dispersity	
DLS	**HDC**	**TEM**	**PSD_{DLS}**	**CV_{HDC} (%)**
11	13	7.5	0.159	10

Stability of PS latex particles. Stability of the PS latex particles is critical to their use in bioapplications, as they have to survive the process that engineers delivery vectors. Stability can be assessed theoretically by knowing the particles surface area coverage. Assuming each of the particle-forming $^{-}$OOC-PAAm-*b*-PS copolymer was 100% chain-extended from HOOC-PAAm chains, the PS core surface area occupied by each steric stabiliser (i.e. PAAm chain) would be equivalent to the area covered by each $^{-}$OOC-PAAm-*b*-PS copolymer chains. Each latex particle core was calculated to be covered by an average of 113 polymer chains, where individual polymer chain was estimated to occupy 1.6 nm^2 of the surface area of the PS core (see ESI for calculations). The average surface area of particle core occupied by each polymer chain was fairly small, suggesting strong sterical stabilization. This steric stability was tested by multiple freeze-thaw cycles, which involved freezing the particle by dry ice at -78.5 °C for an hour, followed by thawing at room temperature – such a process mimics the conditions of storage for delivery vectors. The PSD of the thawed latex was monitored by DLS at the end of each freeze-thaw cycle to detect the presence of aggregates, indicators of unstable particles. The DLS traces in Figure 4 illustrates that no large aggregates were present in the latex during the first five freeze-thaw cycles, indicating the particles remained stable during the freezing process. Starting from the sixth cycle, noticeable amounts of aggregates were detected by DLS. The presence of these aggregates gave rise to PSD of latex from 0.2 to 0.35. The diameter of the particles was observed to increase by approximately 2 nm from the second freeze-thaw cycles. Nevertheless, the particles still demonstrated a good steric stability as major population observed on DLS remained consistent throughout the freeze-thaw cycles.

This suggested the average amount of stabilisers on each particle was sufficient to provide good steric stabilisation for the latex in the aqueous dispersed media.

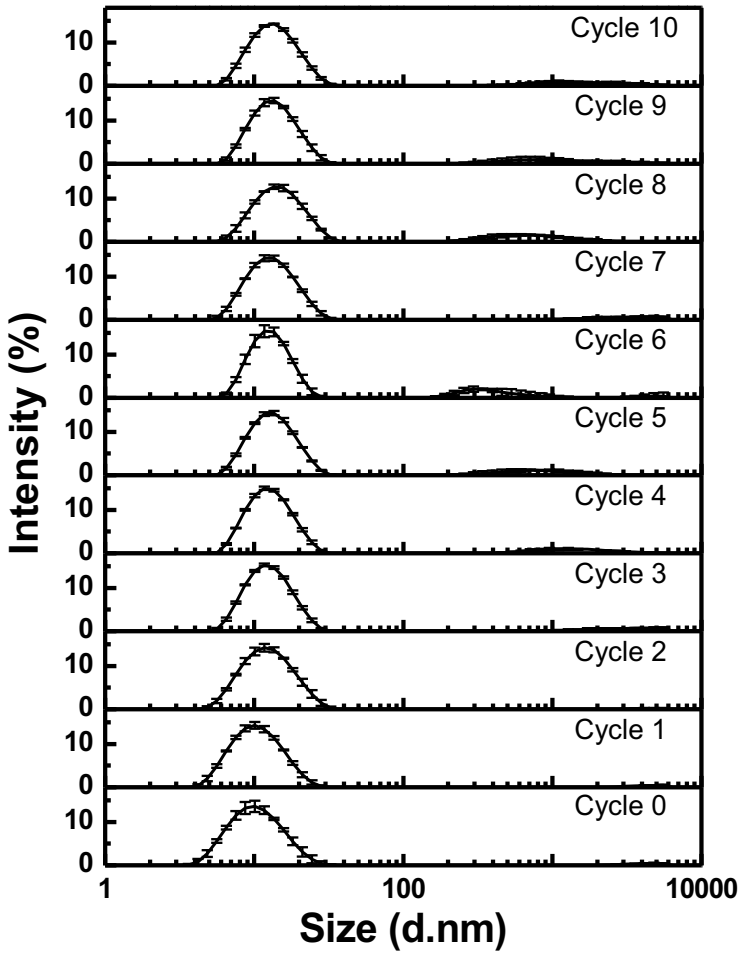

Figure 4. DLS traces of the thawed PS latex particles. 'Cycle 0' represents latex particles without undergoing the freeze-thaw process.

Conjugation of microRNA to PS latex particles. Conjugation of miRNA to the PS latex particles involved a two-step reaction: (1) amidation between amine-bearing 2-(2-pyridyldithio)ethylamine (PDE) linker and carboxylate groups on particle surface, and (2)

thiol-disulfide exchange between PDE linkers on particles and thiol-modified miRNA. This synthetic route was considered to be much cleaner than conjugation in the reversed order as fewer intermediates and side-products would be involved during miRNA attachment.

Conjugation of PDE linker to the latex particles was carried out *via* EDC/NHS coupling. Aiming to modify 20% of the carboxylate groups on the particle surface, the conjugation was carried out by reacting with 0.2 equivalents PDE in the presence of 12 equivalents EDC and 24 equivalents NHS. The conjugation was carried out in 2-(*N*-morpholino)ethanesulfonic acid (MES) buffer at pH 5.65. The use of MES buffer was necessary to maintain the workable pH range for carboxylate activation with EDC. The buffer pH in the activation step, however, was slightly lower than the optimal pH range (pH 6-9) for carboxylic acid esterification with NHS.[43, 44] This condition could prevent complete esterification of the carboxylic acid groups on the particle surface in order to retain the particle stability in water. The amidation was carried out overnight, followed by dialysis to remove unconjugated PDE linkers and by-products from the latex. The modified particles were then treated with reducing agent tris(2-carboxyethyl)phosphine (TCEP) to quantify the amount of PDE loading through the release of pyridinethione, which absorbs at 342 nm.[33] Figure 5 illustrates the UV-Vis spectra of the PDE-loaded PS latex particles during the course of TCEP treatment. The characteristics absorption peak at 310 nm corresponds to the RAFT thiocarbonylthio group on the particles.[45] The slight increase in absorbance at 310 nm was attributed to the release of pyridinethione, which also contributed to the growth of absorbance at 342 nm. The thiocarbonylthio signal did not show any shift of the maximum absorption, indicating the trithiocarbonate groups on the particles remained intact in the presence of TCEP overtime.[46] The PDE conjugation efficiency was calculated to be 19 ± 3.7 %. On average, each particle was functionalised with 4-5 molecules of PDE linkers on the surface.

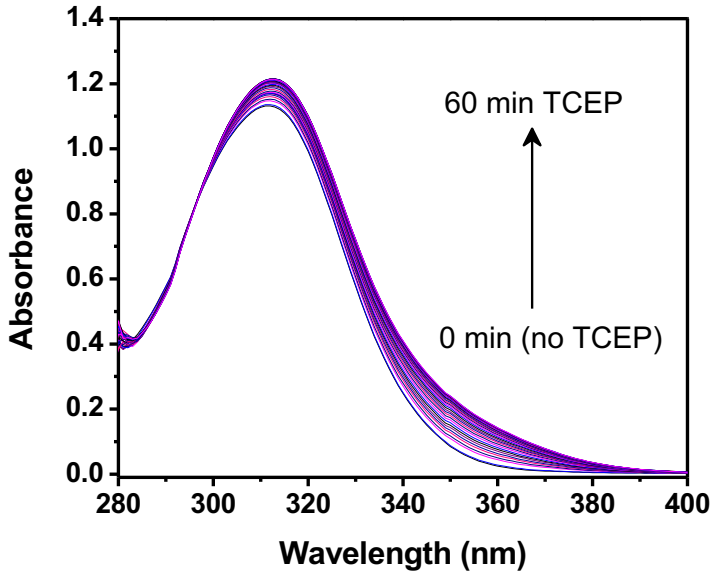

Figure 5. UV-Vis spectra of PDE-loaded PS latex particles after TCEP treatment. The release of pyridinethione upon TCEP reduction was evident by the increase in absorbance between 340 nm and 360 nm over time.

The miRNA model for conjugating to the PS latex particles was a 23-nucleotide long duplex, miR-200b. This miRNA is associated with the decrease in the production of fibronectin, which plays a key role in the development of fibrosis when upregulated.[30] It is anticipated that fibrosis can potentially be treated through therapeutic delivery of miR-200b. Using a duplex is key to the stability of the miRNA, as the incorporation of complementary strand prolonges its intracellular stability when delivered *in vitro* and *in vivo*.[47] The duplex structure can protect the miRNA from pre-mature degradation by ubiquitous endogenous ribonucleases (RNases) prior to loading onto the RNA-induced silencing complex (RISC) in the RNA interference (RNAi) pathway.[48] The 5'-phosphate group of the sense strand, which carried the target miR-200b sequence, was modified with a disulfide group. Reduction of the disulfide with DTT would reveal the thiol functionality at the miRNA end for conjugation to the PDE linkers attached to the particles. Conjugation was performed by mixing the thiol-functionalised miR-

200b to the PDE-modified latex particles at room temperature. The particles, each of which carried at least 4 molecules of PDE linkers on average, reacted with 3 copies of miRNA. The conjugation was followed by UV-Vis and successful miRNA attachment was evident by the increase in absorbance at 342 nm due to the release of pyridinethione. The reaction was stopped after 4 hours when the pyridinethione absorbance became constant. The conjugation proceeded with 86 ± 13% efficiency, which suggested every particle was functionalised with 2-3 copies of miR-200b. The conjugation efficiency was also determined *via* measuring the UV-Vis absorbance of miRNA nucleobases at 260 nm.[49] The miRNA-conjugated PS latex particles were washed by ultrafiltration multiple times to remove unreacted miRNA and pyridinethione. At the end of each wash, the UV-Vis absorbance of the purified particles in the retentate was taken along with the filtrate. Two strong absorption peaks of miRNA nucleobases at 260 nm and RAFT thiocarbonylthio groups on particles at 310 nm were observed from the retentates after each wash **(**Figure 6a**)**. The 260 nm peak shows a gradual decrease in the absorbance due to the removal of unattached miRNA after washing. Nevertheless, the retentate still presented a strong absorbance at 260 nm after five washes, confirming the successful attachment of the nucleic acid to the particles. The free miRNA washed out gave rise to the strong absorbance at 260 nm of the filtrate (Figure 6b**)**. This signal decreased to a low absorbance after the fifth wash, demonstrating most of the unreacted miRNA has been removed. Along with the miRNA signal, the pyridinethione absorption peak at 342 nm was also observed from the filtrate collected after the first wash. The appearance of pyridinethione provided strong evidence for the conjugation to occur *via* thiol-disulfide exchange. The conjugation efficiency was determined from the loss of miRNA in the retentate after the fifth wash and the total amount of miRNA collected in the filtrates. The efficiency calculated from the retentate was 72%, which is close to the value determined from the pyridinethione absorbance within the estimated error. The conjugation efficiency estimated

from the filtrate was found to be 83%, which was similar to the efficiency determined from the pyridinethione approach.

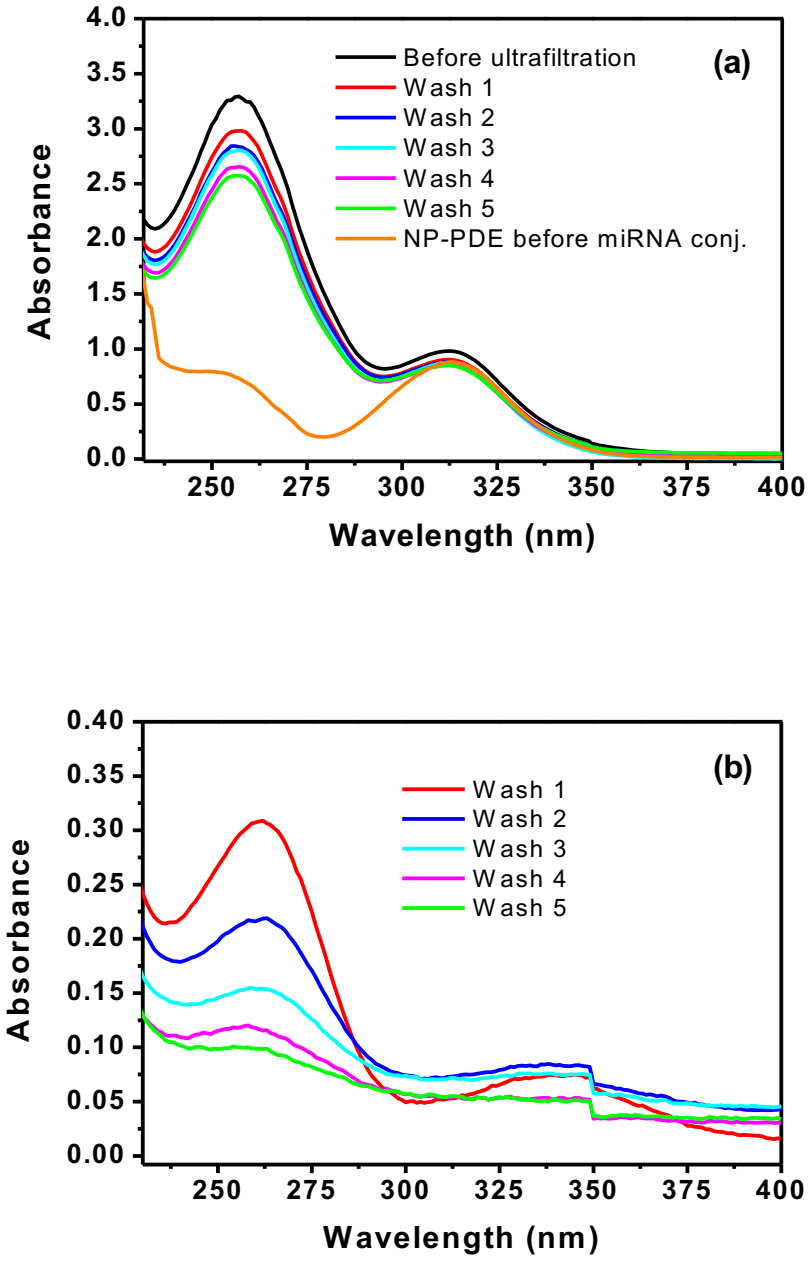

Figure 6. UV-Vis spectra of (a) retentates and (b) filtrates from ultrafiltration of miR-200b-PS latex particles.

Glutathione-triggered miRNA release from miRNA-nanoparticle conjugates. The ability to reduce the disulfide-bridges between the particles and the miRNA was tested with glutathione (GSH). In mammalian cells, the intracellular GSH level ranges between 0.5 mM and 10 mM, which is 1000-fold more concentrated than the extracellular level.[46, 50] Previous studies have demonstrated the slow release of therapeutic agents when the cleavable disulfide-containing vectors were incubated at extracellular GSH concentrations. Near-complete release of the therapeutic agent was achieved within 1 hour when the GSH concentration was increased to the maximum intracellular level.[51-53] Aiming to investigate if the releasing mechanism is as rapid in our system, we incubated the miRNA-nanoparticle conjugates with 10 mM GSH for an hour. The amount of miRNA released was collected by ultrafiltration at 30 and 60 minutes of the incubation and quantified by UV-Vis spectroscopy. The miRNA in the retentates and filtrates was then detected by UV-Vis at 260 nm. The UV-Vis spectra of the retentate with the characteristics miRNA and particle thiocarbonylthio peaks at 260 nm and 310 nm are shown in Figure 7a. The reduction of absorbance at 260 nm signifies some miRNA has been unloaded from the particles in the presence of 10 mM GSH. The release of miRNA was also evident by the sharp increase in the absorbance at 260 nm in the filtrate (Figure 7b). The decrease in miRNA absorbance for the retentate was consistent with the increase in miRNA absorbance for the filtrate. The change in miRNA absorbance was converted in terms of moles to access the amount of detached miRNA. Approximately 10% miRNA has been unloaded from the particles after 30 minute GSH treatment. An additional 10% miRNA was released from the particles when the GSH incubation time was extended to 60 minutes. The miRNA releasing trend was comparable to the work performed by Tzanov and co-workers, who observed 20% of the small interfering RNA (siRNA) on thiolated chitosan nanocapsules was released after incubation with 10 mM GSH for 3 hours. Further incubation of the nanocapsules to 72 hours resulted in a 60% release of the siRNA.[54] The

present system, on the other hand, showed faster kinetics on disulfide bond cleavage by GSH in comparison to the system studied by Lee et al. The disulfide-cross-linked polymeric micelles model employed by Lee exhibited a 17% release of the encapsulated methotrexate after treatment with 10 mM GSH for 25 hours.[55] This difference in the kinetics of disulfide reduction could be explained by the difference in the chemical composition of the drug carriers: high disulfide content requires extended GSH incubation time for complete cleavage, and *vice versa*. Possible explanations for the lack of quantitative release of the miRNA are the poor penetration of GSH into the densely packed polymer shell of the nanoparticles, as well as diffusion of the charged RNA away from the shell where non-specific binding may occur.

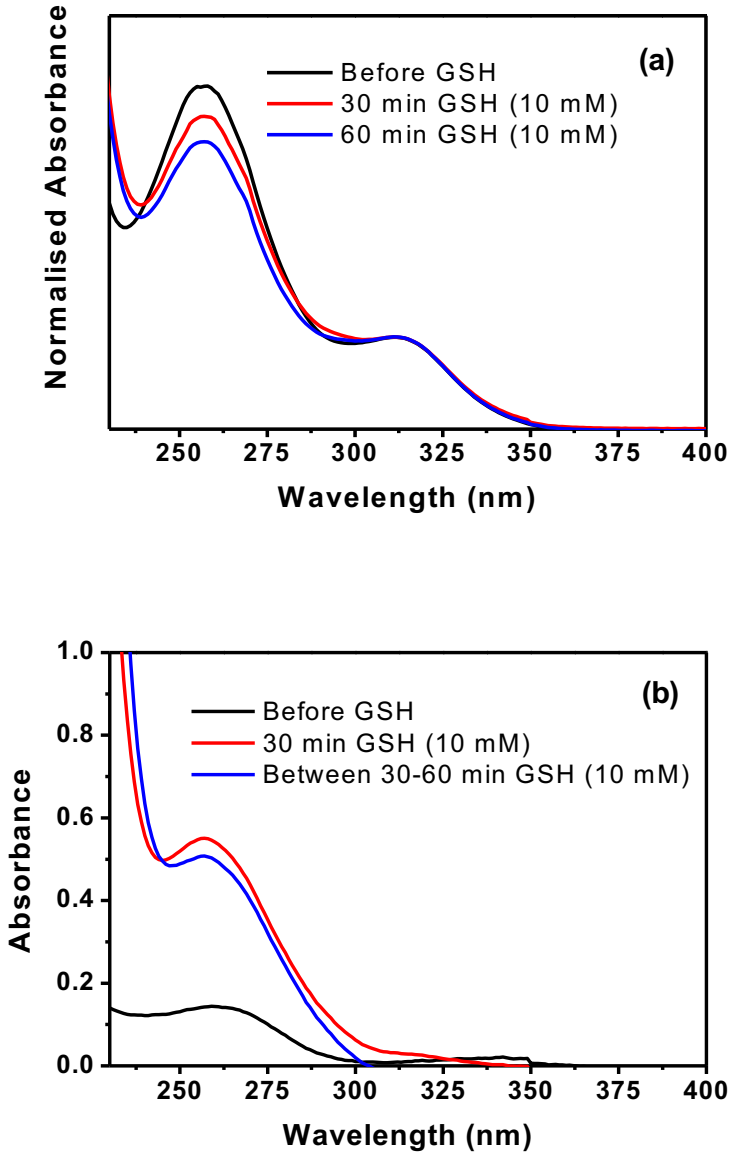

Figure 7. UV-Vis spectra of (a) retentates and (b) filtrates from ultrafiltration of miR-200b-PS latex particles incubated with GSH. The sample before GSH treatment contained traces of unreacted miRNA that has not been removed thoroughly by the previous ultrafiltration.

2.1 Conclusions

We have demonstrated the successful synthesis of amphiphilic HOOC-PAAm$_{14}$-*b*-PS$_8$ diblock copolymer mediated by RAFT polymerisation. The diblock copolymer was able to self-assemble into polymeric micelles for the preparation of 11 nm $^{-}$OOC-PAAm-stabilised latex nanoparticles *via* surfactant-free RAFT emulsion polymerisation. These particles exhibited narrow size distributions as confirmed by DLS, HDC and TEM. Each latex particle core was covered by an average of 113 polymer chains; where individual polymer chain was estimated to occupy 1.6 nm^2 of the surface area of the PS core. The small particle surface area occupied by each polymer chain suggested the particles were well sterically stabilised. Steric stabilisation of particles was further confirmed by their resistance to multiple freeze-thaw cycles. The surface of the sterically stabilised particles was post-polymerization functionalised with 4-5 molecules of PDE linkers *via* EDC/NHS coupling. The PDE linkers attached enabled the conjugation of thiol-modified miR-200b to the particles through thiol-disulfide exchange, which resulted in the attachment of 2-3 copies of the nucleic acid molecules to each particle on average. Incubating the miRNA-conjugated latex with 10 mM GSH for an hour unloaded 20% of the nucleic acid from the particles. The results demonstrated the miRNA-releasing mechanism of the latex particles could be triggered by a biological reducing agent. The particles reported here have a great potential to be used as drug delivery vector. Their small size ensure they can be eliminated and avoid issues with accumulation. The efficiency of the process permit to avoid any residual monomer remain in the colloids, thus avoiding toxicity issues. Beyond drug delivery, we also envision these nanoparticles could be further use, for instance for imaging and diagnostic applications.

Supporting information. ^{1}H NMR and ESI-MS characterisation of macro-RAFT agent, calculation details of livingness of macro-RAT agent, calculation of surface coverage of PS latex particles, 1H NMR characterisation of PDE linker and pyridinethione.

Acknowledgements. The authors wish to thank Dr Algi Serelis (Dulux Group Australia) for the synthesis of the PABTC RAFT agent; Dr Duc Nguyen for obtaining the TEM image of the PS latex particles; Dr Nick Proschogo for PAAm characterisation with ESI-MS; instrumental support from Australian Centre for Microscopy & Microanalysis (TEM) and Dr Deanna D'Alessandro (UV-Vis spectrometer). The authors acknowledge funding from the University of Sydney (CKP, scholarship), the Royal Society Wolfson Merit Award (WM130055; SP) and the Monash-Warwick Alliance (GG; SP).

References

1. Bartlett, D. W.; Davis, M. E., *Bioconjugate Chem.* **2007,** 18, (2), 456-468.

2. Miyata, K.; Nishiyama, N.; Kataoka, K., *Chem. Soc. Rev.* **2012,** 41, (7), 2562-2574.

3. Kanasty, R.; Dorkin, J. R.; Vegas, A.; Anderson, D., *Nat. Mater.* **2013,** 12, (11), 967-977.

4. Elsabahy, M.; Wooley, K. L., *Chem. Soc. Rev.* **2012,** 41, (7), 2545-2561.

5. Chou, L. Y. T.; Ming, K.; Chan, W. C. W., *Chem. Soc. Rev.* **2011,** 40, (1), 233-245.

6. Kamaly, N.; Xiao, Z.; Valencia, P. M.; Radovic-Moreno, A. F.; Farokhzad, O. C., *Chem. Soc. Rev.* **2012,** 41, (7), 2971-3010.

7. Nicolas, J.; Mura, S.; Brambilla, D.; Mackiewicz, N.; Couvreur, P., *Chem. Soc. Rev.* **2013,** 42, (3), 1147-1235.

8. Ferguson, C. J.; Hughes, R. J.; Pham, B. T. T.; Hawkett, B. S.; Gilbert, R. G.; Serelis, A. K.; Such, C. H., *Macromolecules* **2002,** 35, (25), 9243-9245.

9. Ferguson, C. J.; Hughes, R. J.; Nguyen, D.; Pham, B. T. T.; Gilbert, R. G.; Serelis, A. K.; Such, C. H.; Hawkett, B. S., *Macromolecules* **2005,** 38, (6), 2191-2204.

10. Ganeva, D. E.; Sprong, E.; de Bruyn, H.; Warr, G. G.; Such, C. H.; Hawkett, B. S., *Macromolecules* **2007,** 40, (17), 6181-6189.

11. Urbani, C. N.; Monteiro, M. J., RAFT-Mediated Polymerization in Heterogeneous Systems. In *Handbook of RAFT Polymerization*, Wiley-VCH Verlag GmbH & Co. KGaA: 2008; pp 285-314.

12. Chenal, M.; Bouteiller, L.; Rieger, J., *Polym. Chem.* **2013,** 4, (3), 752-762.

13. Rieger, J.; Osterwinter, G.; Bui, C.; Stoffelbach, F.; Charleux, B., *Macromolecules* **2009,** 42, (15), 5518-5525.

14. Rieger, J.; Zhang, W.; Stoffelbach, F.; Charleux, B., *Macromolecules* **2010,** 43, (15), 6302-6310.

15. Chaduc, I.; Girod, M.; Antoine, R.; Charleux, B.; D'Agosto, F.; Lansalot, M., *Macromolecules* **2012,** 45, (15), 5881-5893.

16. Yeole, N.; Hundiwale, D.; Jana, T., *J. Colloid Interface Sci.* **2011,** 354, (2), 506-510.

17. Stoffelbach, F.; Tibiletti, L.; Rieger, J.; Charleux, B., *Macromolecules* **2008,** 41, (21), 7850-7856.

18. Ting, S. R. S.; Min, E. H.; Zetterlund, P. B.; Stenzel, M. H., *Macromolecules* **2010,** 43, (12), 5211-5221.

19. Jiang, G.; Wang, Y.; Zhang, R.; Wang, R.; Wang, X.; Zhang, M.; Sun, X.; Bao, S.; Wang, T.; Wang, S., *ACS Macro Lett.* **2012,** 1, (4), 489-493.

20. Kumarasamy, M.; Kenesei, K.; Li, Y.; Demeter, K.; Kornyei, Z.; Madarasz, E., *Nanoscale* **2015,** 7, 4199-4210.

21. Fleischer, C. C.; Payne, C. K., *Acc. Chem. Res.* **2014,** 47, (8), 2651-2659.

22. Piskin, E.; Tuncel, A.; Denizli, A.; Ayhan, H., *J. Biomater. Sci. Polym. Ed.* **1994,** 5, (5), 451-471.

23. Wu, S.; Shanks, R. A., *J. Appl. Polym. Sci.* **2004,** 93, (3), 1493-1499.

24. Gody, G.; Maschmeyer, T.; Zetterlund, P. B.; Perrier, S., *Macromolecules* **2014,** 47, (2), 639-649.

25. Jiang, J.; Lu, X.; Lu, Y., *J. Polym. Sci. A Polym. Chem.* **2007,** 45, (17), 3956-3965.

26. Becerra-Bracamontes, F.; Sánchez-Díaz, J. C.; González-Álvarez, A.; Ortega-Gudiño, P.; Michel-Valdivia, E.; Martínez-Ruvalcaba, A., *J. Appl. Polym. Sci.* **2007,** 106, (6), 3939-3944.

27. Kanayama, N.; Shibata, H.; Kimura, A.; Miyamoto, D.; Takarada, T.; Maeda, M., *Biomacromolecules* **2009,** 10, (4), 805-813.

28. Bryce, N. S.; Pham, B. T. T.; Fong, N. W. S.; Jain, N.; Pan, E. H.; Whan, R. M.; Hambley, T. W.; Hawkett, B. S., *Biomater. Sci.* **2013,** 1, (12), 1260-1272.

29. Ji, J.; Yan, L.; Xie, D., *J. Polym. Sci. A Polym. Chem.* **2008,** 46, (9), 3098-3107.

30. Tang, O.; Chen, X.-M.; Shen, S.; Hahn, M.; Pollock, C. A., *Am. J. Physiol. Renal Physiol.* **2013,** 304, F1266-F1273.

31. Kanwar, Y.S.; Liu, Z.Z.; Kashihara, N.; Wallner, E.I. *Semin. Nephrol.* **1991**, 11, (4), 390–413.

32. Pham, B. T. T.; Such, C. H.; Hawkett, B. S., *Polym. Chem.* **2015,** 6, (3), 426-435.

33. van der Vlies, A. J.; O'Neil, C. P.; Hasegawa, U.; Hammond, N.; Hubbell, J. A., *Bioconjugate Chem.* **2010,** 21, (4), 653-662.

34. Guryča, V.; Mechref, Y.; Palm, A. K.; Michálek, J.; Pacáková, V.; Novotný, M. V., *J. Biochem. Biophy. Meth.* **2007,** 70, (1), 3-13.

35. Thomas, D. B.; Sumerlin, B. S.; Lowe, A. B.; McCormick, C. L., *Macromolecules* **2003,** 36, (5), 1436-1439.

36. Lowe, A. B.; McCormick, C. L., RAFT Polymerization in Homogeneous Aqueous Media: Initiation Systems, RAFT Agent Stability, Monomers and Polymer Structures. In *Handbook of RAFT Polymerization*, Wiley-VCH Verlag GmbH & Co. KGaA: 2008; pp 235-284.

37. Thomas, D. B.; Convertine, A. J.; Hester, R. D.; Lowe, A. B.; McCormick, C. L., *Macromolecules* **2004,** 37, (5), 1735-1741.

38. Nicolai, T.; Colombani, O.; Chassenieux, C., *Soft Matter* **2010,** 6, (14), 3111-3118.

39. Mai, Y.; Eisenberg, A., *Chem. Soc. Rev.* **2012,** 41, (18), 5969-5985.

40. Siauw, M.; Hawkett, B. S.; Perrier, S., *J. Polym. Sci. A Polym. Chem.* **2012,** 50, (1), 187-198.

41. Bell, N. C.; Minelli, C.; Tompkins, J.; Stevens, M. M.; Shard, A. G., *Langmuir* **2012,** 28, (29), 10860-10872.

42. McDonald, S. A.; Daniels, C. A.; Davidson, J. A., *J. Colloid Interface Sci.* **1977,** 59, (2), 342-349.

43. Lim, C. Y.; Owens, N. A.; Wampler, R. D.; Ying, Y.; Granger, J. H.; Porter, M. D.; Takahashi, M.; Shimazu, K., *Langmuir* **2014,** 30, (43), 12868-12878.

44. Hermanson, G. T., Chapter 4 - Zero-Length Crosslinkers. In *Bioconjugate Techniques (Third edition)*, Hermanson, G. T., Ed. Academic Press: Boston, 2013; pp 259-273.

45. Skrabania, K.; Miasnikova, A.; Bivigou-Koumba, A. M.; Zehm, D.; Laschewsky, A., *Polym. Chem.* **2011,** 2, (9), 2074-2083.

46. Phillips, D. J.; Patterson, J. P.; O'Reilly, R. K.; Gibson, M. I., *Polym. Chem.* **2014,** 5, (1), 126-131.

47. Raemdonck, K.; Remaut, K.; Lucas, B.; Sanders, N. N.; Demeester, J.; De Smedt, S. C., *Biochemistry* **2006,** 45, (35), 10614-10623.

48. Raemdonck, K.; Vandenbroucke, R. E.; Demeester, J.; Sanders, N. N.; De Smedt, S. C., *Drug Discov. Today* **2008,** 13, (21–22), 917-931.

49. Voet, D.; Gratzer, W. B.; Cox, R. A.; Doty, P., *Biopolymers* **1963,** 1, (3), 193-208.

50. Meister, A.; Anderson, M. E., *Annu. Rev. Biochem.* **1983,** 52, 711-760.

51. Kim, J. O.; Sahay, G.; Kabanov, A. V.; Bronich, T. K., *Biomacromolecules* **2010,** 11, (4), 919-926.

52. Navath, R. S.; Kurtoglu, Y. E.; Wang, B.; Kannan, S.; Romero, R.; Kannan, R. M., *Bioconjugate Chem.* **2008,** 19, (12), 2446-2455.

53. Kurtoglu, Y. E.; Navath, R. S.; Wang, B.; Kannan, S.; Romero, R.; Kannan, R. M., *Biomaterials* **2009,** 30, (11), 2112-2121.

54. Francesko, A.; Fernandes, M. M.; Perelshtein, I.; Benisvy-Aharonovich, E.; Gedanken, A.; Tzanov, T., *J. Mater. Chem. B* **2014,** 2, (36), 6020-6029.

55. Koo, A. N.; Lee, H. J.; Kim, S. E.; Chang, J. H.; Park, C.; Kim, C.; Park, J. H.; Lee, S. C., *Chem. Commun.* **2008**, (48), 6570-6572.